

OBJECT-ORIENTED MONITORING OF FOREST DISTURBANCES WITH ALOS/PALSAR TIME-SERIES

Charles Marshak^{1}, Marc Simard¹, and Michael Denbina¹*

¹ Jet Propulsion Laboratory, California Institute of Technology, Pasadena, CA 91109, USA

ABSTRACT

We present a flexible methodology to identify forest loss in synthetic aperture radar (SAR) L-band ALOS/PALSAR images. Instead of single pixel analysis, we generate spatial segments (i.e., superpixels) based on local image statistics to track homogeneous patches of forest across a time-series of ALOS/PALSAR images. Forest loss detection is performed with Support Vector Machines (SVMs) trained on local radar backscatter features derived within superpixels. This method is applied to time-series of ALOS-1 and ALOS-2 radar images over a boreal forest within the Laurentides Wildlife Reserve in Québec. We evaluate four spatial arrangements including 1) single pixels, 2) square grid cells, 3) superpixels based on segmentation of the radar images, and 4) superpixels derived from ancillary optical imagery (e.g. Landsat). Detection of forest loss with superpixels outperform single pixel and regular grid methods, especially when superpixels are generated from ancillary optical imagery. Results are validated with official Québec forestry data and Hansen forest loss products. Our results indicate that this approach may be applied operationally to monitor forests across large study areas with L-band radar instruments such as ALOS/PALSAR.

Index Terms— Change Detection; Forest Disturbance; PALSAR; L-band SAR; Microwave Remote Sensing

1. INTRODUCTION

Tracking forest disturbance is an important part of carbon monitoring and ecological modeling. L-band images have been shown to be a valuable data source for forest monitoring [1]. There is continued interest in L-band land cover and land use change analysis with the current ALOS-2 and SAO-COM missions, and the forthcoming ALOS-3 NISAR missions, which will provide high temporal and spatial resolution imagery. An important NISAR objective is to monitor forest disturbances at the 1 ha scale [2].

We present a methodology for detecting forest disturbance from L-band SAR time-series. Given a time-series of images

(i.e., image stack), our method identifies when and where forest disturbance occurred. In determining when a change occurred, we consider a small window of images around a particular date and extract a temporally averaged pair. Using this pair, we apply a two-part change detection method. First, with a segmentation of our image, we derive backscatter features. Then, we use a classifier to determine if a segment lost forest.

In this work, we consider a simple pair of features: the initial backscatter and the backscatter change. It is well known that a decrease in HV backscatter may indicate forest loss [1]. We use linear γ in our methodology and aggregate segment statistics in these units.

Superpixel segmentation has become an increasingly important tool for change detection [1]. For our segmentation procedure, we employ the superpixel methodology of [3]. We use the mean backscatter within a segment to characterize a superpixel as a proxy for individual pixel backscatter. Superpixel analysis speeds up processing as there are less superpixels to analyze than pixels. Further, superpixel segments track changes at a larger spatial scale than individual pixels. We evaluate 4 different local spatial contexts or shapes in our change analysis: specifically, we evaluate superpixels derived from backscatter, superpixels derived from optical products, square cells derived from a regular grid, and individual pixels. As we show in Section 3, superpixels are better suited to track image changes than segments generated by a square grid of comparable size as well as individual pixel analysis. Moreover, we find that superpixels derived from ancillary optical products may improve our change analysis further.

Once feature vectors have been extracted, we need a classifier to determine if change has occurred. One can directly apply an unsupervised classifier as in [4], a statistical test as in [5] or apply a Markov Random Field to further incorporate spatial relationships [6]. We take a supervised approach and train an SVM similar to [7].

2. METHODOLOGY

In this section, we describe our methodology for change detection on SAR image stacks to identify forest loss. First, we discuss the preprocessing of an image stack. Then, we discuss our change detection methodology.

This research was carried out at the Jet Propulsion Laboratory, California Institute of Technology, under a contract with the National Aeronautics and Space Administration. ©2019, California Institute of Technology. Government sponsorship acknowledged

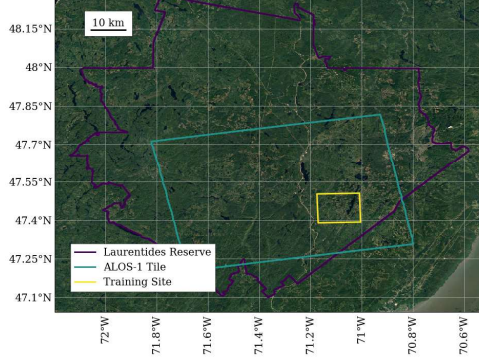


Fig. 1: The Laurentides Wildlife Reserve (shown with the purple line), and the ALOS-1 tile used as the dataset for this study (shown in teal).

Preprocessing our image stack is crucial to mitigate environmental and phenological effects. In this work, we consider two different stacks: HV ALOS-1 image tiles radiometrically corrected for terrain (i.e. RTC corrected) by the ASF [8] and HV ALOS-2 image tiles RTC processed with [9]. We select images acquired from June through September during peak biomass and to avoid snow cover.

Once we have a set of RTC images, we project all the images into the same coordinate reference and remove no data pixels consistently. With a spatially coregistered and correctly masked stack, we perform channel by channel preprocessing. First, we clip the dynamic range of our HV image to fall between -30 and -5 dB. Then, we apply total variation (TV) denoising [10] in dB to remove noise. Although SAR noise in dB is additive and γ -distributed [11], we empirically found that TV denoising works well, which assumes noise is Gaussian. We used weight parameter $\lambda = .25$ for ALOS-1 and $\lambda = .5$ for ALOS-2 (see [10] for parameter description). We found this denoising works better for segmentation than a Gaussian filter [3] and the denoised image stack can be used for subsequent analysis.

To complete preprocessing, we adjust image statistics through large superpixels. Specifically, we normalize a pixel’s backscatter p at image index i according to

$$\hat{p}_i = (p_i - \mu_i) \frac{\sigma_0}{\sigma_i} + \mu_0,$$

where μ_i, σ_i are the i^{th} ’s image’s mean and standard deviation, respectively, within the segment the pixel p belongs. Because ALOS/PALSAR tiles span such a large area, a similar normalization through the entire image produced poor results. Our superpixel-based normalization method is more robust in the presence of spatial variation within a ALOS/PALSAR tile, for example due to changes in vegetation moisture content in different parts of the study area. We select segments that are approximately 2 orders of magnitude larger than the smallest change we wish to observe (in this work, 2 ha is the mini-

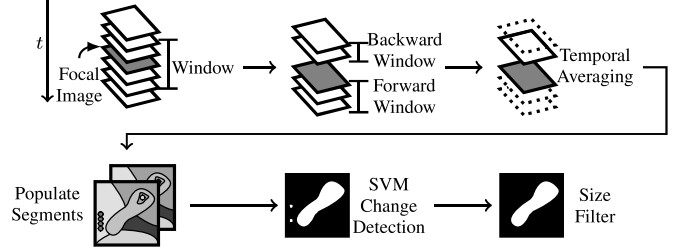


Fig. 2: Schematic for Change Detection Pipeline

um change we wish to observe). To acquire such segments, we increased minimum size m and the scale κ both by 2 orders of magnitude from the ones we expect to use in change analysis (see [3] for parameter description).

We now describe the change detection methodology. The change detection outputs a map indicating regions of disturbance and the date that they were disturbed. We assume each region is disturbed at most once. We frequently refer to forest loss as “disturbance” or “change”.

To determine if change occurred in a particular image I_j of our stack, we first select a window around this image. We call I_j the *focal image* of our window. We specify a forward window and backward window as in Figure 2. The window sizes w_f and w_b determine the temporal scale we wish to consider. A longer window size means the changes should be observable at longer time scales. For our analysis of forest loss, we typically ensure that each window spans a few years (we used $w_b = w_f = 2$ for ALOS/PALSAR images). Within a window, we average the images within the forward and backward window, respectively. We are left with an image pair to perform change detection. These first steps of our change analysis are summarized in the first row of the flow chart in Figure 2.

Next, we introduce superpixel segments [3] to our change analysis. From these segments, we derive mean backscatter and mean backscatter change between the forward and backward windows. We extract these superpixels using the first and the last images in our stack. We found that selecting minimum size m to be 10 pixels and scale κ to be 0.1 for ALOS-1 and ALOS-2 HV backscatter images produced quality segments with mean size approximately .25 ha. We generally found this was the smallest size for quality segments without changing the image contrast significantly given the resolution of the images. Even though these segments are still sensitive to speckle noise, our size filter effectively removed small false positives. Further, finer segments are able to better capture disturbance boundaries. Because of the segment sizes we used, we consider changes at modestly larger scale than [2] as higher resolution change maps were less reliable. We also select elementary segment features because the resulting decision boundary for our change analysis is easily interpreted.

With these elementary segment features, we load a trained

SVM with a radial basis function as our model’s kernel [12] to determine where changes occur. We trained our model on a pair of images over a small study area where there was visible forest loss. In Figure 1, we show the extent of the training area. We trained our models using available validated forestry data consistent with the ALOS/PALSAR time-series. Because there are far more “change” than “no change” segments, we select a random sample of “no change” segments to overcome the class imbalance. We ensemble 50 models together (each trained on a different random sample) to remove sample dependence. With a trained SVM, we identify change within a temporally averaged pair. To remove regions of small, isolated changes, we apply a size filter, removing changed areas that are smaller than 2 ha. We summarize the entire change detection methodology in Figure 2.

3. APPLICATIONS

In this section, we apply our change methodology to ALOS/PALSAR time series. We illustrate good results given that some forest disturbances are not visible in SAR images and the ground truth data is imperfect. We also show the lift of tracking regions with superpixels over both segments generated by a square grid with comparable size and individual pixels. For our application, we consider a pair of images from ALOS-1 and ALOS-2 stacks trained using well-known forest disturbance data [13, 7]. We train an SVM on a small subset of the full Laurentides tile and then validate each methodology on the full tile. After we discuss the performance of the methodology using superpixels, square segments, and individual pixels, we apply the methodology and trained model to the full time-series to illustrate the proposed data product.

3.1. ALOS-1

We now apply our change methodology to an ASF-processed ALOS-1 stack [8]. We train and validate our methodology using open Québec data [13] produced by the forestry service. We consider only four types of forest disturbances: total cuts, cuts with protection of *small* or *high* merchantable stems and soil, and cuts with regeneration protection (see [13]). These correspond to approximately 85% of all disturbances and are visible over the training area we selected. Because we apply a size filter to our final change map, we remove changes within this dataset whose total area is below 2 ha.

The Québec data, in addition to providing when and where disturbance occurred, also provides a segmentation of the ALOS-1 tile, so we train our model using these segments directly. We also apply our trained model to these segments as an additional point of comparison. Because the forest loss data is based on the Québec segments, our methodology does best using these segments. These segments, which were created using aerial photographs, allows us to incorporate optical image information into SAR analysis. We note the F_1

Segments	F_1	Prod. Acc.	User Acc.
Quebec Segments	0.7719	0.6871	0.8806
Superpixels	0.597	0.5377	0.6709
Pixels	0.571	0.5131	0.6436
Squares	0.567	0.5044	0.6473

Table 1: ALOS-1 tile results

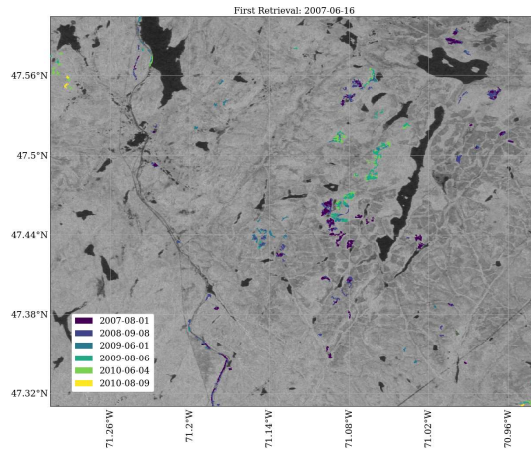


Fig. 3: A detailed area of the tile, including the expansion of route 175 [14] in the bottom of the image.

score of the other segmentations over our training area are all roughly the same ($\approx .7 \pm .01$). In Table 1, we compare changes tracked using superpixels, square segments, and individual pixels on the full ALOS-1 tile. We show the F_1 score, the producer accuracy, and user accuracy using the forestry data as ground truth. Superpixels perform the best after the Québec segments. The main source of mislabeling comes from false positives, which includes the expansion of Route 175 [14] requiring the cutting of trees along this highway but not included in the Québec forestry data.

Using our trained ensemble of models, we identify disturbance in the full ALOS-1 stack illustrated in Figure 3. We see the expansion of Route 175 at the bottom of the image [14].

3.2. ALOS-2

We now describe our change analysis on an ALOS-2 stack over the same area. We use Hansen forest disturbance data [7] to train our model as Québec forestry data does not go past 2014. We performed radiometric terrain correction with [9]. We modify the original Hansen forest loss map so training is done on segments rather than pixels, mitigating speckle and improving efficiency. First, we extracted superpixels from Hansen’s 2017 landsat mosaic. Then, with the changes that aligned with our ALOS-2 retrieval dates, we labeled a segment as change if a majority of pixels within the extracted segments were changed. This ensured that segments with a

Segments	F_1	Prod. Acc.	User Acc.
Landsat Segments	0.5169	0.5329	0.5019
Superpixels	0.4841	0.5098	0.4609
Pixels	0.4668	0.4672	0.4665
Squares	0.458	0.4371	0.481

Table 2: ALOS-2 results.

high volume of forest loss were trained correctly. Since regions labeled as undisturbed are randomly sampled during training, we expect false negatives to be of minor impact during training. However, when validating our model on the full ALOS-2 tile, we used the original Hansen change map with losses smaller than 2 ha filtered out. We proceed with the same change analysis as in Section 3.2. Table 2 compares the change methodology on the Landsat segments, superpixels, square segments, and individual pixels, illustrating that the superpixels derived from Landsat do for change detection.

4. CONCLUSIONS

We have introduced a flexible change detection methodology for identifying forest loss in ALOS/PALSAR images and validate the methodology with official Québec forestry data [13] and Hansen forest loss products [7]. Our methodology uses simple features so that this change method can be adapted for other forest sites and other L-band image stacks. We demonstrate the use of superpixel segmentation in our change analysis to improve computational efficiency, reduce speckle, and incorporate optical information. We compare superpixel segmentation within our change methodology favorably to segments generated by a square grid cells and individual pixels. Further, we illustrate how spatial segmentation can be used to incorporate optical data into our SAR change analysis to improve change detection accuracy. In future work, we plan to compare more spatial segmentation methods in addition to expand our methodology to create change maps over multiple tiles for larger studies.

5. REFERENCES

- [1] M. Shimada, T. Itoh, T. Motooka, M. Watanabe, T. Shiraishi, R. Thapa, and R. Lucas, “New global Forest/Non-Forest Maps from ALOS PALSAR Data (2007–2010),” *Remote Sensing of Environment*, vol. 155, pp. 13–31, 2014.
- [2] NISAR Science Team, “NASA-ISRO SAR Mission Science Users Handbook,” https://nisar.jpl.nasa.gov/files/nisar/NISAR_Science_Users_Handbook.pdf, 2019, [Online; accessed January-2019].
- [3] P. F. Felzenszwalb and D. P. Huttenlocher, “Efficient Graph-based Image Segmentation,” *International Journal of Computer Vision*, vol. 59, no. 2, pp. 167–181, 2004.
- [4] T. Celik, “Unsupervised Change Detection in Satellite Images using Principal Component Analysis and k -means Clustering,” *IEEE Geoscience and Remote Sensing Letters*, vol. 6, no. 4, pp. 772–776, 2009.
- [5] A. A. Nielsen, “The Regularized Iteratively Reweighted MAD Method for Change Detection in Multi- and Hyper-Spectral Data,” *IEEE Transactions on Image processing*, vol. 16, no. 2, pp. 463–478, 2007.
- [6] L. Bruzzone and D. F. Prieto, “Automatic Analysis of the Difference Image for Unsupervised Change Detection,” *IEEE Transactions on Geoscience and Remote sensing*, vol. 38, no. 3, pp. 1171–1182, 2000.
- [7] M. C. Hansen, P. V. Potapov, R. Moore, M. Hancher, S. A. A. Turubanova, A. Tyukavina, D. Thau, S. V. Stehman, S. J. Goetz, T. R. Loveland *et al.*, “High-resolution Global Maps of 21st Century Forest Cover Change,” *Science*, vol. 342, no. 6160, pp. 850–853, 2013.
- [8] Alaska Satellite Facility, “Asf daac 2015; includes material ©JAXA/METI 2007,” <http://dx.doi.org/10.5067/Z97HFCNKR6VA>.
- [9] M. Simard, B. V. Riel, M. Denbina, and S. Hensley, “Radiometric Correction of Airborne Radar Images over Forested Terrain with Topography,” *IEEE Transactions on Geoscience and Remote Sensing*, vol. 54, no. 8, pp. 4488–4500, 2016.
- [10] L. I. Rudin, S. Osher, and E. Fatemi, “Nonlinear Total Variation Based Noise Removal Algorithms,” *Physica D: Nonlinear Phenomena*, vol. 60, no. 1-4, pp. 259–268, 1992.
- [11] J. M. Bioucas-Dias and M. A. T. Figueiredo, “Multiplicative Noise Removal Using Variable Splitting and Constrained Optimization,” *IEEE Transactions on Image Processing*, vol. 19, no. 7, pp. 1720–1730, 2010.
- [12] B. E. Boser, I. M. Guyon, and V. N. Vapnik, “A Training Algorithm for Optimal Margin Classifiers,” in *Proceedings of the 5th Annual Workshop on Computational Learning Theory*. ACM, 1992, pp. 144–152.
- [13] Ministry of Forests, Wildlife and Parks, “Ecoforest Map With Disturbances.”
- [14] Quebec Transportation, “Route 73/175 Project,” https://web.archive.org/web/20110716214657/http://www.mtq.gouv.qc.ca/portal/page/portal/grands_projets/trouver_grand_projet/axe_routier_73_175, 2008, [Online; accessed December-2018].